Stability of thin-shell structures and imperfection sensitivity analysis with the Asymptotic Numerical Method

Sébastien Baguet, Bruno Cochelin

Stability of thin-shell structures and imperfection sensitivity analysis with the Asymptotic Numerical Method

Sébastien Baguet — Bruno Cochelin

Laboratoire de Mécanique et d'Acoustique CNRS UPR 7051
Ecole Supérieure de Mécanique de Marseille
IMT Technopôle de Château Gombert
13451 Marseille Cedex 20
{baguet,cochelin}@mn.esm2.imt-mrs.fr

ABSTRACT. *This paper is concerned with stability behaviour and imperfection sensitivity of thin elastic shells. The aim is to determine the reduction of the critical buckling load as a function of the imperfection amplitude. For this purpose, the direct calculation of the so-called fold line connecting all the limit points of the equilibrium branches when the imperfection varies is performed. This fold line is the solution of an extended system demanding the criticality of the equilibrium. The Asymptotic Numerical Method is used as an alternative to Newton-like incremental-iterative procedures for solving this extended system. It results in a very robust and efficient path-following algorithm that takes the singularity of the tangent stiffness matrix into account. Two specific types of imperfections are detailed and several numerical examples are discussed.*

RÉSUMÉ. *Ce travail concerne la stabilité des coques minces élastiques et leur sensibilité aux imperfections. L'objectif est la détermination de la courbe de réduction de charge critique de flambement en fonction de l'amplitude de l'imperfection. Pour cela, on procède à un calcul direct de la courbe de suivi de point limites qui relie tous les points limites des branches d'équilibre lorsque l'imperfection varie. Cette courbe de suivi est solution d'un système augmenté qui caractérise les points d'équilibre singuliers. La résolution de ce système augmenté est effectuée à l'aide de la Méthode Asymptotique Numérique qui est une alternative aux méthodes incrémentales itératives de type Newton. L'algorithme de suivi de branche qui en résulte est très robuste et très performant et prend en compte la singularité de la matrice de rigidité tangente. Deux types d'imperfections sont détaillés et plusieurs exemples sont traités.*

KEYWORDS: *Buckling, thin shells, imperfection sensitivity, fold line, extended system, Asymptotic Numerical Method, finite elements.*

MOTS-CLÉS : *Flambement, coques minces, sensibilité aux imperfections, courbe de suivi de points limites, système augmenté, Méthode Asymptotique Numérique, éléments finis.*

1. Introduction

The development of new materials and the wide use of optimization techniques over the past decades have conducted to very thin and slender structures. Since structural stability is a question of prime interest for such structures, a considerable attention has been given to the development of efficient numerical algorithms for the description of the post-buckling path and the treatment of bifurcation and limit points which provide the critical buckling load (see figure 1). In the case of quasi-static linear elasticity, the underlying post-buckling problem can be represented by the discretized geometrically non-linear equation

$$F(u,\lambda) = f(u) - p(\lambda) = 0 \qquad [1]$$

which expresses the balance between internal forces and external forces. The internal forces depend only on the current displacement vector u where u is a N-dimensional vector, i.e. contains N dof's. The external forces are assumed to be proportional to an external loading F_e and take the form $p(\lambda) = \lambda F_e$ where λ is the load parameter. The solution of [1] is usually obtained by an incremental-iterative procedure such as the Newton-Raphson method [RIK 72, CRI 81] which is commonly implemented in standard commercial FEM codes. However, alternative procedures for solving nonlinear problems in structural mechanics, like the Asymptotic Numerical Method (ANM) [DAM 90, AZR 93, COC 94b] or the LATIN method [LAD 98], can also be used.

For slender structures, a stability analysis is all the more complex that they are often very sensitive to imperfections. A small defect can significantly reduce their critical buckling load, causing the collapse for a smaller value than in the perfect case (without imperfection). A simple way for carrying a sensitivity analysis consists in introducing an imperfection in the definition of the structure and in solving problem [1] for this "imperfect" structure. Doing so, an equilibrium branch is obtained for each

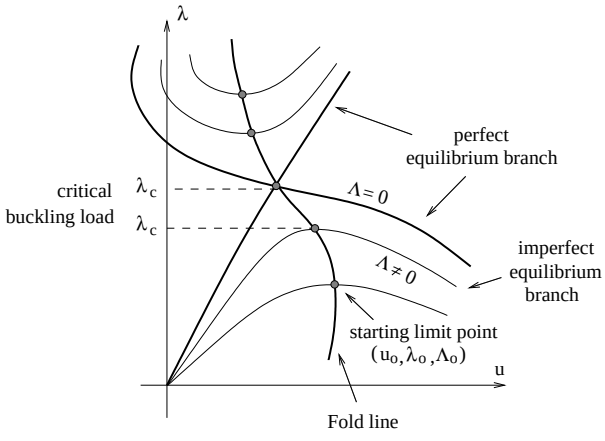

Figure 1. *Perfect and imperfect equilibrium paths and fold line*

value of the imperfection amplitude Λ, as represented in figure 1, and the limit point on each of them gives the "imperfect" buckling load. This type of analysis is very simple to implement and the previously described algorithms can be used.

Nevertheless, this procedure is not the most suitable for a sensitivity analysis. Indeed, this succession of re-analyses is very costly since a full computation on the structure is required for each requested limit point. Moreover, it provides informations only for the few imperfection amplitudes that have been fixed. In practice, it is not judicious to calculate all the different equilibrium paths. It is more advisable to determine precisely a starting critical state for a given imperfection amplitude, and then to follow directly the fold line connecting all the limit points when the imperfection varies (see figure 1). By this way, it is not necessary to compute all the equilibrium paths. Only the fold line is computed. To this end, the imperfection amplitude Λ must become an additional parameter in the governing equations. In this paper we will only consider shape and thickness imperfections . Thus, only the internal forces are affected and the previous one-parameter system [1] becomes a two-parameter system which reads

$$F(u, \lambda, \Lambda) = f(u, \Lambda) - \lambda F_e = 0 \qquad [2]$$

The solution of this system is now a load-imperfection-displacement surface which is made of the load-displacement curves for all the possible values of the imperfection amplitude. On this surface, we are only interested in the limit points with respect to λ. In order to isolate these limit points, a constraint equation characterizing the criticality of the equilibrium is appended to the equilibrium equations. The two-parameter nonlinear system [2] is then transformed into a so-called "augmented" or "extended" system which reads

$$H\left(u, \lambda, \Lambda\right) = \left(\begin{array}{c} F\left(u, \lambda, \Lambda\right) \\ G\left(u, \Lambda\right) \end{array} \right) = 0 \qquad [3]$$

The solution of this extended system is restricted to the fold-line that directly gives the reduction of the critical buckling load when the imperfection varies.

2. Augmented problem

Many alternatives concerning the constraint equation $G\left(u, \Lambda\right) = 0$ have been proposed in the literature. The simplest of them is based on the study of the determinant of the tangent stiffness matrix $K_T = F_{,u}$, where the notation $F_{,u}$ indicates the differentiation of F with respect to u, but this criterium is not well suited for a numerical implementation. Another criterium which is more efficient from a numerical point of view is also based on the appearance of a null eigenvalue for the tangent stiffness matrix K_T at simple critical states but it does not require the computation of the determinant. The right null vector ϕ associated with the null eigenvalue of K_T is used instead, yielding the following constraint equation

$$G\left(u, \Lambda\right) = F_{,u}\left(u, \Lambda, \lambda\right) \cdot \phi = K_T(u, \Lambda) \cdot \phi = 0 \qquad [4]$$

With this expression for the additional constraint equation, the extended system [3] can be rewritten as

$$H\left(u,\phi,\Lambda,\lambda\right)=\left(\begin{array}{c} F\left(u,\Lambda,\lambda\right) \\ F_{,u}\left(u,\Lambda,\lambda\right)\cdot\phi \\ \|\phi\|-1 \end{array}\right)=\left(\begin{array}{c} f\left(u,\Lambda\right)-\lambda F_e \\ K_T(u,\Lambda)\cdot\phi \\ \|\phi\|-1 \end{array}\right)=0 \qquad [5]$$

The last normalization equation on ϕ is added to ensure the uniqueness of the solution and to avoid numerical problems by preventing ϕ from becoming excessively large or small.

In the context of structural mechanics, this extended system has been first introduced by Keener and Keller [KEE 73]. It has subsequently been studied or used by Moore and Spence [MOO 80], Weinitschke [WEI 85], Wriggers *et al.* [WRI 88] and Wriggers and Simo [WRI 90], among others, for the precise calculation of limit and simple bifurcation points in the case of perfect structures. Indeed, in this particular case ($\Lambda = 0$), the solution of [3] is restricted to a single point. The mathematical study of [3] with Λ varying has been carried out by Jepson and Spence [JEP 85] and it has been numerically investigated by Eriksson [ERI 94] and Deml and Wunderlich [DEM 97] for sensitivity analyses, in a finite element framework and using incremental-iterative strategies.

3. Asymptotic algorithm for the fold line following

In this paper, the sensitivity analysis is reconsidered using the so-called Asymptotic Numerical Method (ANM) as an alternative to classical incremental-iterative methods. This method is inspired by the perturbation techniques which were developed by Thompson and Walker [THO 68] for decomposing a nonlinear problem into a sequence of linear ones. These perturbation techniques have been revisited and efficiently solved by means of the finite element method by Cochelin, Damil and Potier-Ferry [DAM 90, AZR 93, COC 94b]. Since the solution obtained with the ANM is valid only in the vicinity of the starting point, a continuation method has been proposed by Cochelin [COC 94a], allowing a curve to be described in a step by step way.

The ANM has two major advantages. On one hand, its computational cost is reduced as compared to the incremental-iterative methods because the continuation procedure requires less tangent stiffness matrix decompositions. On the other hand, the continuation method is very robust and reliable. It allows to follow very complicated paths without jumping on other branches as it can happen with the Newton-Raphson method when the length of the predictor step is not carefully set. With the ANM, the step length is based on the equilibrium residual and can be computed a posteriori. By this way, it is guaranteed to be always optimal for each continuation step and no special procedure is needed for its resizing.

This method can be used for solving a large class of problems involving smooth or strong nonlinearities. For a non-exhaustive list, the interested reader should refer to

[POT 97, NAJ 98]. An original bifurcation indicator based on the ANM has been proposed by Boutyour [BOU 95, BAG 00] for the precise detection of simple bifurcations and limit points and for the calculation of the associated eigenmode. Supposing that a starting limit point has been isolated by means of this algorithm, the direct following of the fold line is performed as follows with the ANM.

We assume that the solution $(u, \phi, \lambda, \Lambda)$ of the extended system [5] can be represented by a truncated power series expansion with respect to an additional parameter a

$$\begin{array}{l} u(a) = u_0 + a\,u_1 + a^2\,u_2 + \ldots + a^n\,u_n \\ \phi(a) = \phi_0 + a\,\phi_1 + a^2\,\phi_2 + \ldots + a^n\,\phi_n \\ \Lambda(a) = \Lambda_0 + a\,\Lambda_1 + a^2\,\Lambda_2 + \ldots + a^n\,\Lambda_n \\ \lambda(a) = \lambda_0 + a\,\lambda_1 + a^2\,\lambda_2 + \ldots + a^n\,\lambda_n \end{array} \qquad [6]$$

where the point $(u_0, \phi_0, \Lambda_0, \lambda_0)$ is known. In fact, it corresponds to the previously isolated limit point which is used as a starting point. This starting point is a singular point of the equilibrium equation F, like every point of the fold line, but it is a regular point of the extended system H. These series expansions depend on the path parameter a. Because of this new variable, an additional constraint equation is needed. By analogy with the classical arc-length method, we choose the following definition for a

$$a = (u - u_0).u_1 + (\Lambda - \Lambda_0)\Lambda_1 + (\lambda - \lambda_0)\lambda_1 \qquad [7]$$

The next step consists in introducing the series expansions [6] into the nonlinear extended system [5] and in the definition of a [7]. By identifying the terms with the same power of a, one obtains a succession of linear problems and the problem at order 1 reads

$$\left[\begin{array}{cccc} K_T & 0 & F_1 & -F_e \\ K_\phi & K_T & F_2 & 0 \\ 0 & \phi_0^T & 0 & 0 \\ u_1^T & 0 & \Lambda_1 & \lambda_1 \end{array}\right] \left[\begin{array}{c} u_1 \\ \phi_1 \\ \Lambda_1 \\ \lambda_1 \end{array}\right] = \left[\begin{array}{c} 0 \\ 0 \\ 0 \\ 1 \end{array}\right] \begin{array}{c} (N \text{ eq.}) \\ (N \text{ eq.}) \\ (1 \text{ eq.}) \\ (1 \text{ eq.}) \end{array} \qquad [8]$$

The solution $(u_1, \phi_1, \Lambda_1, \lambda_1)$ of this linear system is the tangential direction of the fold line at the starting point $(u_0, \phi_0, \Lambda_0, \lambda_0)$. This system is exactly the same as for the predictor step of the Newton-Raphson method [ERI 99, DEM 97]. Indeed, the matrix K_ϕ et the two vectors F_1 and F_2 correspond to the differentials of the mapping F evaluated at the starting point $(u_0, \phi_0, \Lambda_0, \lambda_0)$

$$K_T(u_0, \Lambda_0) = f_{,u}(u_0, \Lambda_0) \qquad [9]$$

$$K_\phi(u_0, \phi_0, \Lambda_0) = f_{,uu}(u_0, \Lambda_0) \cdot \phi_0 \qquad [10]$$

$$F_1(u_0, \Lambda_0) = f_{,\Lambda}(u_0, \Lambda_0) \qquad [11]$$

$$F_2(u_0, \phi_0, \Lambda_0) = f_{,u\Lambda}(u_0, \Lambda_0) \cdot \phi_0 \qquad [12]$$

As pointed out by several authors [ERI 99], the accuracy of these derivatives are of paramount importance for the efficiency of the algorithm because they are used to define the properties of the solution. Nevertheless, since an analytical calculation of

these differentials is often a very painful task, a numerical approximation is usually preferred [WRI 90, REI 95]. In the present case, with the use of the ANM, exact analytical forms of these differentials can be easily obtained. Since the introduction of series expansions into a set of equations acts as a linearization tool, the directional derivatives with respect to the expanded variables follow from the identification of the power-like terms. Moreover, provided that the equations are written in a quadratic framework, the asymptotic expansions can easily be computed. The different steps that lead to the extended system [8] at order 1 and provide K_T, K_ϕ, F_1 and F_2 are described in appendix I. It must also be noted that, because of the differentiation with respect to Λ, the vectors F_1 and F_2 depend on the type of imperfection (shape or thickness in the present paper) whereas the matrices K_T and K_ϕ do not.

Equating power-like terms at order p ($p \leq n$) yields the following system

$$\begin{bmatrix} K_T & 0 & F_1 & -F_e \\ K_\phi & K_T & F_2 & 0 \\ 0 & \phi_0^T & 0 & 0 \\ u_1^T & 0 & \Lambda_1 & \lambda_1 \end{bmatrix} \begin{bmatrix} u_p \\ \phi_p \\ \Lambda_p \\ \lambda_p \end{bmatrix} = \begin{bmatrix} F_p^{nl} \\ G_p^{nl} \\ h_p^{nl} \\ 0 \end{bmatrix} \begin{matrix} (N \text{ eq.}) \\ (N \text{ eq.}) \\ (1 \text{ eq.}) \\ (1 \text{ eq.}) \end{matrix} \qquad [13]$$

The tangent augmented matrix is the same as for order 1. Only the r.h.s. terms are different. These terms contain the non-linearities of the problem. They are fully determined because they depend only on the solution at previous orders $(u_r, \phi_r, \lambda_r, \Lambda_r)$ with $r < p$. As a result, recursively solving the succession of linear augmented systems will provide all the coefficients of the series [6]. The r.h.s. terms depend on the considered type of imperfection and, as for the differentials [9]-[12], analytical expressions follow from the identification process. For lack of space, their expression will not be given here. The interested reader can refer to [BAG 01] for more details about their calculation.

In practice, a deflated block elimination is used to solve the extended system [13] in order to consider only subsystems of size N involving the matrix K_T. Such a block-elimination scheme can be found in Wriggers and Simo [WRI 90]. Its main interest relies on the fact that only the classical matrix K_T needs to be decomposed, thus saving a large amount of calculation time. Besides this particular procedure, another numerical difficulty must be pointed out. Since all the solution points of H are singular ones of F, the matrix K_T is singular all along the fold line connecting the computed solution points. That means that the classical matrix decomposition techniques cannot be used. A special procedure based on Lagrange multipliers is introduced to bypass this problem. A detailed description of the adaptation of the block-elimination and Lagrange multipliers procedures to the system [13] is given in [BAG 00].

Because of the limited radius of convergence of the series, only a fraction of the solution curve is obtained. Indeed, the accuracy of the solution deteriorates very quickly when the radius of convergence is reached. A criterium that gives the length of a step has been proposed by Cochelin [COC 94a]. Its justification is given in [BAG 01]. This criterium is based on the study of the residual of equilibrium equations [2]. In the case of our extended system, both residuals of the first and second equations of [5] must be

monitored. However, numerical experiments have shown that the second equation is always more accurate than the first one. As a result, the classical criterium based on the equilibrium residual can be used. According to this criterium, for series truncated at order n, the maximal value of the path parameter a for which the solution satisfies a requested accuracy ε is given by

$$a_M = \left(\frac{\varepsilon}{\|F_{n+1}^{nl}\|} \right)^{\frac{1}{n+1}} \qquad [14]$$

Using this formula, the step length is set after all the coefficients of the series have been computed. By this way, the step length is guaranteed to be optimal. Once the step has been stopped, the starting point is updated and the global procedure is restarted. Thus, the solution curve is described in a step by step way, as it would be with the classical continuation algorithms. The strong point of this procedure is its robustness. Furthermore, it is completely automatic from the user's point of view. The only parameters that need to be chosen are the order n of the series and the accuracy ε. Setting n equal to 20 or 30 and $\varepsilon = 10^{-5}$ is often a good compromise.

4. Numerical results

The following examples are concerned with a cylindrical panel submitted to a concentrated load at its top. The geometrical and material properties and the boundary conditions of the panel are defined in Figure 2a. Using symmetry conditions, only a quarter of the panel was considered for the calculations and a 10×10 mesh with 200 triangular DKT shell elements [BAT 92] and 726 degrees of freedom was used. The aim of these examples is to analyse the sensitivity of the critical buckling load of the cylindrical panel to a thickness or a shape imperfection, i.e. to calculate the fold line for both cases. Using the Asymptotic Numerical Method, the equilibrium branch was first evaluated for a thickness h=6.35mm. The well-known results of this academic test are reported in Figure 2b. The equilibrium branch exhibits two limit points (one maximum and one minimum) associated with the snap-through behaviour of the panel. These limit points can subsequently be used as starting points for the fold line following. With an accuracy $\varepsilon = 10^{-5}$ and series at order 30, this equilibrium curve was obtained with only 12 ANM continuation steps, i.e. with only 12 decompositions of the tangent stiffness matrix K_T.

4.1. *Cylindrical panel with thickness imperfection*

In this first example, the thickness h is chosen as the additional parameter Λ in order to carry out a sensitivity analysis with respect to the thickness of the panel. This can be used for example to study the influence of corrosion on the stability of the structure. A starting limit point was first isolated for an initial value of the thickness h=12.7mm and then the fold line was followed using the Asymptotic Numerical

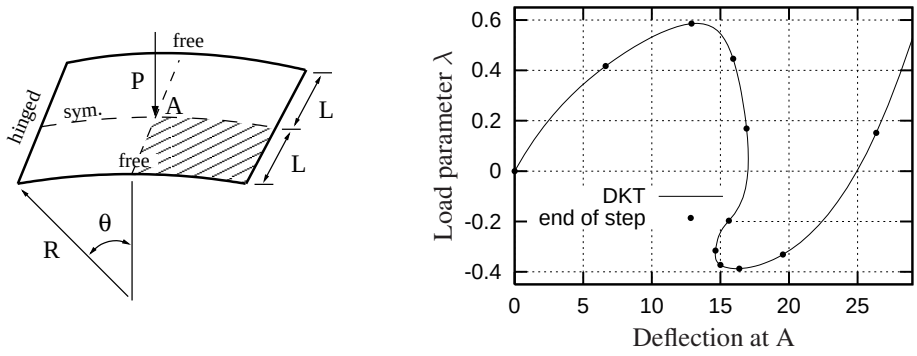

Figure 2. *(a) Geometrical and material properties of the cylindrical panel: R=2540mm, L=254mm, θ=0.1rad, thickness h=6.35mm, E=3102.75 MPa, ν=0.3 (b) Equilibrium curve of the perfect cylindrical panel.*

Method as described in previous sections. The "load-deflection-thickness" 3D representation of this fold line as well as the associated projections are plotted in Figure 3. Only 20 ANM continuation steps with series at order 30, i.e. only 20 decompositions of the tangent stiffness matrix K_T, were needed to describe the entire fold line. The end of each continuation step is represented by a dot in figure 3.

The two most interesting projections of the fold line are shown in figures 4 and 5. In figure 4 the fold line as well as two equilibrium curves (for h=12.7mm and h=22.15mm) with their associated limit points are plotted. As expected, the fold line intersects the equilibrium branches at their two limit points (maximum and minimum),

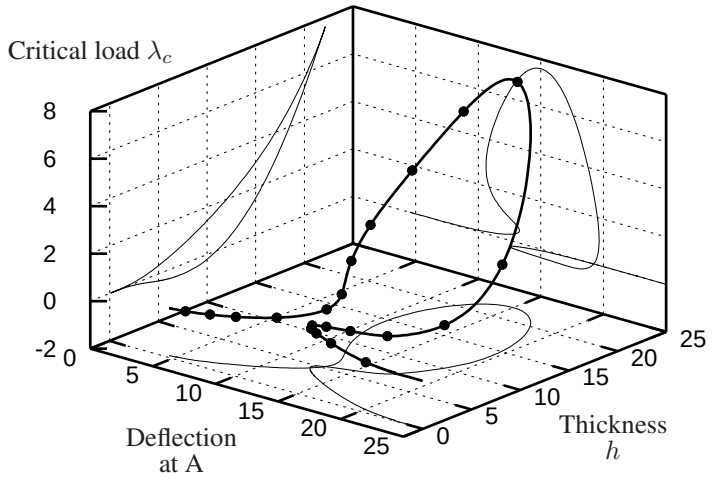

Figure 3. *Projections and 3D representation of the fold line.*

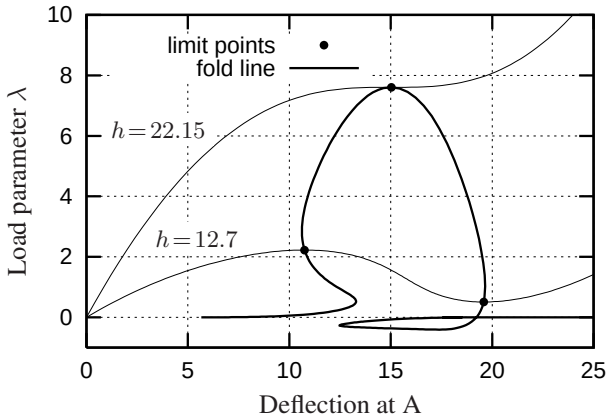

Figure 4. *Fold line and equilibrium curves with associated limit points for different values of the thickness ($h=12.7$ and $h=22.15$)*

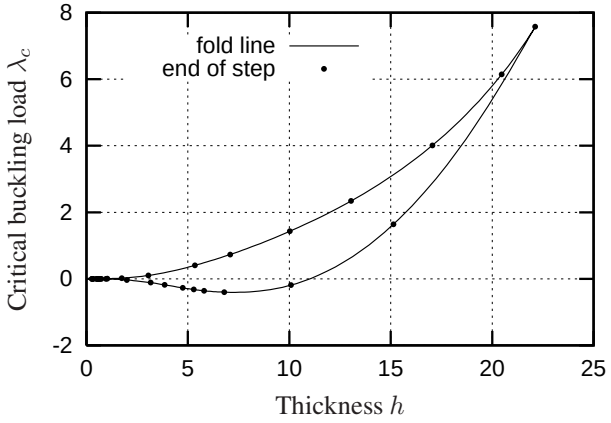

Figure 5. *Reduction of the critical buckling load with respect to the thickness.*

excepted for the extreme value $h\simeq 22.15$ of the thickness for which the two limit points merge into an inflection point and exchange their role. Beyond this value, there is no snap-through phenomenon anymore. This behaviour can also be observed on figure 5 which shows the critical buckling load as a function of the panel thickness. For a given thickness, this curve gives the critical buckling load corresponding to the maximum and the minimum limit points of the equilibrium branches of figure 4. It can also clearly be inferred from this curve that there is no limit point beyond the value $h\simeq 22.15$. The results obtained here are in very good agreement with those obtained by Eriksson et al. in [ERI 99].

Most of the time, only a part of the fold line in the neighbourhood of a given imperfection amplitude is needed. In that case, it is not useful to compute the entire fold

line. The following strategy, as illustrated in figure 6, is preferable. A starting limit point was isolated for a value of the thickness close to h=22.15. Then the fold line was followed in the neighbourhood of this value. Since the series expansions [6] are valid for positive or negative values of the path parameter a, the fold line can be followed in the two directions with the same series. Moreover, the series expansions can beneficially be replaced by rational representations called Padé approximants. The extra calculation cost is very small and the range of validity of the series is usually doubled [COC 94c, ELH 00]. The results obtained with Padé approximants are plotted in figure [6]. The previously computed, complete fold line is also plotted as a reference. No continuation was used for Padé approximants, only one step is represented here, and no residual criterium was used to stop the step. So, one can see their range of validity. With only one decomposition of the tangent matrix K_T and the use of Padé approximants, the fold line is valid from $h\simeq$22.15 to $h\simeq$12.7. Beyond this value, the solution is out of the range of validity and the curve deviates from the reference fold line.

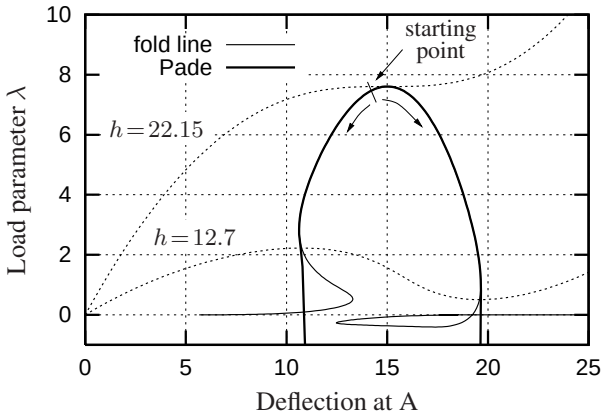

Figure 6. *Series improvement with Padé approximants.*

4.2. *Cylindrical panel with shape imperfection*

The second example refers to the same cylindrical panel, with geometrical and material properties as defined in figure 2. The aim is now to analyse the sensitivity of its

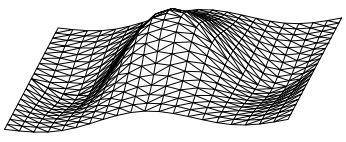

Figure 7. *First buckling mode of the panel without imperfection.*

critical buckling load to a geometrical shape imperfection. The first buckling eigenmode of the panel is shown in Figure 7. It was normalized by setting the greatest value of its displacement to 1 in order to provide the shape of the considered geometrical imperfection. The additional scalar parameter Λ is now used to monitor the amplitude of the shape imperfection. The notation η will be used instead of Λ in the sequel.

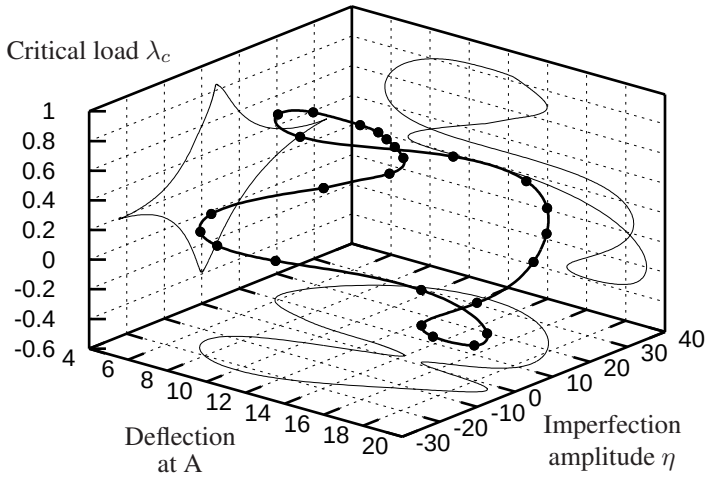

Figure 8. *Projections and 3D representation of the "load-displacement-imperfection" fold line.*

For this example, the starting point was evaluated for an initial imperfection amplitude η_0=-3mm, i.e. -0.47 times the thickness (h=6.35mm) of the panel. The curve shown in figure 8 is a 3D representation of the resulting fold line connecting all the limit points when the imperfection varies. This is a closed curve. Its projections are more suitable for our analysis. Two of them are represented in figures 9 and 10. The first projection is located in the load-deflection plane. Three equilibrium branches are plotted for different values of the imperfection as well as the projection of the fold line. The fold line intersects each equilibrium branch at its two limit points. The equilibrium branch of figure 9 for the perfect panel (η=0) is represented here again as a reference. The values of the load at its two limit points (maximum and minimum) can be also read on the right-hand-side figure 10 which gives the critical buckling load reduction with respect to the imperfection. The top and bottom parts of this curve correspond respectively to the variation of the maximum and minimum limit point of the equilibrium curves. The curve shows that the two limit points get closer when the imperfection amplitude increases. For two extreme values $\eta\simeq$-3.5h and $\eta\simeq$5.3h of the imperfection, the limit points merge and exchange their role. Beyond these extreme values, there is no limit point anymore, i.e. no snap-through phenomenon anymore. It can be noted that the entire fold line was computed with only 25 continuation steps, i.e. only 25 tangent matrix decompositions.

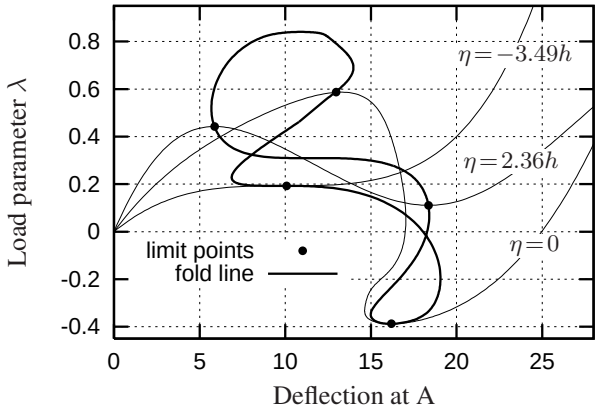

Figure 9. *Fold line and equilibrium curves with associated limit points for different values of the imperfection amplitude ($\eta = 0$, $\eta = 2.36h$ and $\eta = -3.49h$).*

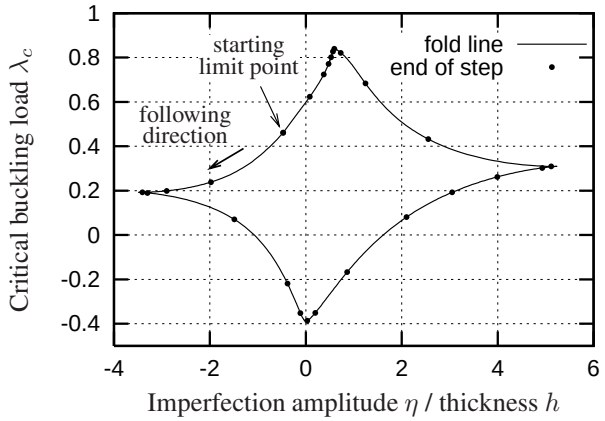

Figure 10. *Reduction of the critical buckling load with respect to the amplitude of the shape imperfection.*

5. Conclusions

This paper has described a general procedure for the imperfection sensitivity analysis of elastic structures. The developed calculation tool can handle global as well as local imperfections, in the case of thickness or geometrical shape defects.

The Asymptotic Numerical Method is used for the numerical treatment of the problem. As a result, the required calculation cost is significantly reduced as compared to the classical Newton-Raphson procedure. Moreover, the geometrical nonlinearities are treated without any approximation and exact analytical expressions are obtained

for the directional derivatives of the tangent stiffness matrix. Thus, no approximation is introduced and the resulting overall algorithm is very accurate and the continuation procedure is very robust.

In order to deal with more complex structures, future developments will concern the implementation of a shell element which handles large rotations. Material nonlinearities will also be introduced. Nevertheless, because of the dependance to the loading history, plasticity with unloading phenomenon can not be considered for the fold line following and the only possible nonlinear constitutive laws are be restricted to nonlinear elasticity. In the case of plastic buckling, an alternative strategy to the fold line following must be used. Such a strategy can be found for example in [LEG 02].

6. References

[AZR 93] AZRAR L., COCHELIN B., DAMIL N., POTIER-FERRY M., "An asymptotic numerical method to compute the post-buckling behavior of elastic plates and shells", *International Journal for Numerical Methods in Engineering*, vol. 36, 1993, p. 1251-1277.

[BAG 00] BAGUET S., COCHELIN B., "Direct computation of paths of limit points using the Asymptotic Numerical Method", *IASS-IACM 2000, 4th International Colloquium on Computation of Shell & Spatial Structures*, Chania - Crete, Greece, June 5-7 2000.

[BAG 01] BAGUET S., "Stabilité des structures minces et sensibilité aux imperfections par la Méthode Asymptotique Numérique", Mémoire de Thèse de Doctorat, École Supérieure de Mécanique de Marseille, Université d'Aix-Marseille II, 2001.

[BAT 92] BATOZ J., DHATT G., *Modélisation des structures par éléments finis*, vol. 1,2,3, Hermès, Paris, 1992.

[BOU 95] BOUTYOUR E., "Détection des bifurcations par des méthodes asymptotiques-numériques", *Deuxième colloque national en calcul des structures*, vol. 2, Giens, France, May 1995, p. 687-692.

[COC 94a] COCHELIN B., "A path following technique via an asymptotic numerical method", *Computers & Structures*, vol. 29, 1994, p. 1181-1192.

[COC 94b] COCHELIN B., DAMIL N., POTIER-FERRY M., "The Asymptotic-Numerical-Method: an efficient perturbation technique for nonlinear structural mechanics", *Revue Européenne des Éléments Finis*, vol. 3, 1994, p. 281-297.

[COC 94c] COCHELIN B., DAMIL N., POTIER-FERRY M., "Asymptotic-Numerical Methods and Pade approximants for nonlinear elastic structures", *International Journal for Numerical Methods in Engineering*, vol. 37, 1994, p. 1181-1192.

[CRI 81] CRISFIELD M., "A fast incremental/iterative solution procedure that handles "snap-through"", *Computers & Structures*, vol. 13, 1981, p. 55-62.

[CRI 97] CRISFIELD M., *Non-linear finite element analysis of solids and structures*, vol. 2, Wiley, New York, 1997.

[DAM 90] DAMIL N., POTIER-FERRY M., "A new method to compute perturbed bifurcations: application to the buckling of imperfect elastic structures", *International Journal of Engineering Sciences - N9*, vol. 28, 1990, p. 943-957.

[DEM 97] DEML M., WUNDERLICH W., "Direct evaluation of the 'worst' imperfection shape in shell buckling", *Computer Methods in Applied Mechanics and Engineering*, vol. 149, 1997, p. 201-222.

[ELH 00] ELHAGE-HUSSEIN A., POTIER-FERRY M., DAMIL N., "A numerical continuation method based on Padé approximants", *International Journal of Solids and Structures*, vol. 37, 2000, p. 6981-7001.

[ERI 94] ERIKSSON A., "Fold lines for sensitivity analyses in structural instability", *Computer Methods in Applied Mechanics and Engineering*, vol. 114, 1994, p. 77-101.

[ERI 99] ERIKSSON A., PACOSTE C., ZDUNEK A., "Numerical Analysis of complex instability behaviour using incremental-iterative strategies", *Computer Methods in Applied Mechanics and Engineering*, vol. 179, 1999, p. 265-305.

[JEP 85] JEPSON A., SPENCE A., "Folds in solutions of two parameter systems and their calculation. Part I", *S.I.A.M. Journal of numerical analysis*, vol. 22, 1985, p. 347-368.

[KEE 73] KEENER J., KELLER H., "Perturbed bifurcation theory", *Archives for Rational Mechanics and Analysis*, vol. 50, 1973, p. 159-179.

[LAD 98] LADEVÈZE P., *Nonlinear Computational Structural Mechanics*, Springer-Verlag, New York, 1998.

[LEG 02] LEGAY A., COMBESCURE A., "Efficient algorithms for parametric non-linear instability analysis", *International Journal of Non-linear Mechanics*, vol. 37, 2002, p. 709-722.

[MOO 80] MOORE G., SPENCE A., "The calculation of turning points of nonlinear equations", *S.I.A.M. Journal of numerical analysis*, vol. 17, 1980, p. 567-576.

[NAJ 98] NAJAH A., COCHELIN B., DAMIL N., POTIER-FERRY M., "A critical review of Asymptotic Numerical Methods", *Archives of Computational Methods in Engineering*, vol. 5, 1998, p. 31-50.

[POT 97] POTIER-FERRY M., DAMIL N., BRAIKAT B., DESCAMPS J., CADOU J., CAO H., ELHAGEHUSSEIN A., "Traitement des fortes non-linéarités par la méthode asymptotique numérique", *Compte Rendu de l'Académie des Sciences*, vol. t 314, 1997, p. 171-177, Serie II b.

[REI 95] REITINGER R., RAMM E., "Buckling and imperfection sensitivity in the optimization of shell structures", *Thin-Walled Structures*, vol. 23, 1995, p. 159-177.

[RIK 72] RIKS E., "The application of Newton's method to the problem of elastic stability", *Journal of Applied Mechanics, Transactions of A.S.M.E*, vol. 39, 1972, p. 1060-1066.

[THO 68] THOMPSON J., WALKER A., "The nonlinear perturbation analysis of discrete structural systems", *International Journal of Solids and Structures*, vol. 4, 1968, p. 757-758.

[WEI 85] WEINITSCHKE H., "On the calculation of limit and bifurcation points in stability problems of elastic shells", *International Journal of Solids and Structures*, vol. 21, num. 1, 1985, p. 79-95.

[WRI 88] WRIGGERS P., WAGNER W., MIEHE C., "A quadratically convergent procedure for the calculation of stability points in finite element analysis", *Computer Methods in Applied Mechanics and Engineering*, vol. 70, 1988, p. 329-347.

[WRI 90] WRIGGERS P., SIMO J., "A general procedure for the direct calculation of turning and bifurcation points", *International Journal for Numerical Methods in Engineering*, vol. 30, 1990, p. 155-176.

Appendix I : Directional derivatives of F

In this appendix, the procedure for obtaining the directional derivatives K_T, K_ϕ, F_1 and F_2 is presented for both shape and thickness imperfections.

In the case of geometrical nonlinear elasticity, [1] is cubic with respect to u. This cubic expression is not very suitable for asymptotic expansions. A quadratic expression is preferred. It is achieved by introducing the stress-strain relation as an additional equation. [1] can thus be replaced by the following equivalent system

$$F(u,\lambda) = \left\{ \begin{array}{l} \displaystyle\int_\Omega B^T(u)\, S\, dV - \lambda F_e = 0 \\ \quad S = D\, \left(B_l + \tfrac{1}{2} B_{nl}(u)\right)\, u \end{array} \right. \qquad [15]$$

We have used the classical B operator defined by $B(u)=B_l+B_{nl}(u)$ where B_l and $B_{nl}(u)$ are the classical operators expressing the linear and nonlinear parts of the Green-Lagrange strain [CRI 97]. S is the second Piola Kirchhoff stress operator and D is the classical elasticity operator function. The first equation stands for equilibrium. It is quadratic with respect to the set of variables (u, S). The constitutive law has been introduced in order to make both equations quadratic. The additional equation [4] is then obtained by differentiation with respect to u and reads

$$F_{,u}\,(u,\lambda)\cdot\phi = \left\{ \begin{array}{l} \displaystyle\int_\Omega B^T(u)\,\Psi + B^T_{nl}(\phi)\, S\, dV = 0 \\ \quad \Psi = D\, \left(B_l + B_{nl}(u)\right)\, \phi \end{array} \right. \qquad [16]$$

where Ψ is the stress associated with the eigenvector ϕ.

Appendix I.1 : Geometrical shape imperfection

In order to get a scalar extra parameter, the imperfection is written as

$$u^\star = \eta\, u_0^\star \qquad [17]$$

where $u_0^\star$ is a fixed displacement which gives the shape of the imperfection and η is its amplitude. With these notations, the introduction of the imperfection transforms equations [15] and [16] into

$$F(u,\eta,\lambda) = \left\{ \begin{array}{l} \displaystyle\int_\Omega B^T(u)\, S + \eta\, B^T_{nl}(u_0^\star)\, S\, dV - \lambda F_e = 0 \\ \quad S = D\, \left(B_l + \tfrac{1}{2} B_{nl}(u) + \eta\, B_{nl}(u_0^\star)\right)\, u \end{array} \right. \qquad [18]$$

$$F_{,u}\,(u,\eta,\lambda)\cdot\phi = \left\{ \begin{array}{l} \displaystyle\int_\Omega B^T(u)\,\Psi + \eta\, B^T_{nl}(u_0^\star)\,\Psi + B^T_{nl}(\phi)\, S\, dV = 0 \\ \quad \Psi = D\, \left(B_l + B_{nl}(u) + \eta\, B_{nl}(u_0^\star)\right)\, \phi \end{array} \right. \qquad [19]$$

The next step consists in introducing the series expansions [6] of u, S, ϕ, Ψ, η and λ into [18] and [19]. The identification of the terms with the same power of a gives at order 1

$$\begin{cases} \displaystyle\int_\Omega \tilde{B}_0^T\, S_1 + B_{nl}^T(u_1)\, S_0 + \eta_1\, B_{nl}(u_0^\star)\, S_0\, dV = \lambda_1 F_e \\ \quad S_1 = D\, \left(\tilde{B}_0\, u_1 + \eta_1\, B_{nl}(u_0)\, u_0^\star\right) \end{cases} \quad [20]$$

$$\begin{cases} \displaystyle\int_\Omega \tilde{B}_0^T\, \Psi_1 + B_{nl}^T(\phi_1)\, S_0 + B_{nl}^T(u_1)\, \Psi + \eta_1\, B_{nl}^T(u_0^\star)\, \Psi_0 + B_{nl}^T(\phi_0)\, S_1\, dV = 0 \\ \quad \Psi_1 = D\, \left(\tilde{B}_0\, \phi_1 + B_{nl}(\phi_0)\, (u_1 + \eta_1\, u_0^\star)\right) \end{cases} \quad [21]$$

where $\tilde{B}_0 = B(u_0 + \eta_0 u_0^\star)$ is introduced to shorten the notations. In order to go back to a displacement formulation, S_1 and Ψ_1 are then replaced in equations $[20]_1$ and $[21]_1$. These variables were introduced only to make the asymptotic expansions easier. Finally, the problem at order 1 can be written in the following form

$$K_T\, u_p + \eta_p\, F_1 = \lambda_p\, F \quad [22]$$

$$K_\phi\, u_p + K_T\, \phi_p + \eta_p\, F_2 = 0 \quad [23]$$

which corresponds to the two first lines of [8] with

$$K_t = \int_\Omega \tilde{B}_0^T\, D \tilde{B}_0 + G^T \hat{S}_0 G\, dV \quad [24]$$

$$K_\phi = \int_\Omega \tilde{B}_0^T\, D\, B_{nl}(\phi_0) + B_{nl}^T(\phi_0)\, D\, \tilde{B}_0 + G^T\, \hat{\Psi}_0\, G\, dV \quad [25]$$

$$F_1 = \int_\Omega \left(\tilde{B}_0^T\, D\, B_{nl}(u_0) + G^T\, \hat{S}_0\, G\right)\, u_0^\star\, dV \quad [26]$$

$$F_2 = \int_\Omega \left(\tilde{B}_0^T\, D\, B_{nl}(\phi_0) + B_{nl}^T(\phi_0)\, D\, B_{nl}(u_0) + G^T\, \hat{\Psi}_0\, G\right)\, u_0^\star\, dV \quad [27]$$

Appendix I.2 : Thickness imperfection

In this section, the additional parameter is the thickness of the shell. For simplicity, we focus on shell finite elements which are analytically integrated through the thickness, and where the thickness explicitly appears only in the elasticity matrix D. The DKT18 shell element [BAT 92] is an example of such an element. For this class of shell elements, the elasticity matrix $D(h) = D^1\, h + D^3\, h^3$ can be decomposed into a membrane part and into a bending part, which are respectively linear and cubic with respect to h. According to $[15]_2$ and the definition of D, the constitutive law is quadratic with respect to u and cubic with respect to h. Since the asymptotic expansions are easier in a quadratic framework, we introduce some additional variables in

order to reduce the order of the equations and to turn them into a quadratic form. This is achieved as follows

$$F(u,h,\lambda) = \begin{cases} \int_\Omega B^t(u)\, S\, dV - \lambda F_e = 0 \\ S = D\,\gamma \\ \gamma = \left(B_l + \frac{1}{2}B_{nl}(u)\right)\, u \\ D = D^1\, h + D^3\, eh \\ e = h^2 \end{cases} \quad [28]$$

$$F_{,u}\,(u,h,\lambda)\cdot\phi = \begin{cases} \int_\Omega B^t(u)\,\Psi + B^t_{nl}(\phi)\, S\, d\Omega = 0 \\ \Psi = D\,\varepsilon \\ \varepsilon = (B_l + B_{nl}(u))\,\phi \end{cases} \quad [29]$$

Through the introduction of the variables S, γ, Ψ, ε and e, each equation of the previous systems is quadratic. By this way, the number of products which follow from the introduction of the series will be significantly reduced. Each of the variables u, S, γ, ϕ, Ψ, ε, D, e, h and λ is then expanded into a power series and replaced in [28] and [29], yielding at order 1

$$\begin{cases} \int_\Omega B^T(u_0)\, S_1 + B^T_{nl}(u_1)\, S_0\, dV = \lambda_1 F_e \\ S_1 = D_0\,\gamma_1 + D_1\,\gamma_0 \\ \gamma_1 = B(u_0)\, u_1 \\ D_1 = D^1\, h_1 + D^3\, e_0 h_1 + D^3\, e_1 h_0 \\ e_1 = 2h_0 h_1 \end{cases} \quad [30]$$

$$\begin{cases} \int_\Omega B^T(u_0)\,\Psi_1 + B^T_{nl}(\phi_1)\, S_0 + B^T_{nl}(u_1)\,\Psi_0\, dV = 0 \\ \Psi_1 = D_0\,\varepsilon_1 + D_1\,\varepsilon_0 \\ \varepsilon_1 = B(u_0)\,\phi_1 + B_{nl}(\phi_0)\, u_1 \end{cases} \quad [31]$$

The successive elimination of all the additional variables in [30] is performed as follows. e_1 is first substituted into D_1, then D_1 and γ_1 are replaced into S_1 and finally S_1 is reported into the equilibrium equation. Applying the same process to [31] yields again equations [22] and [23], but this time F_1 and F_2 read

$$F_1 = \int_\Omega B_0^T\, \tilde{D}\, (B_l + \tfrac{1}{2}B_{nl}(u_0))\, u_0\, dV \quad [32]$$

$$F_2 = \int_\Omega B_0^T\, \tilde{D}\, B_0\, \phi_0 + B^T_{nl}(\phi_0)\, \tilde{D}\, (B_l + \tfrac{1}{2}B_{nl}(u_0))\, u_0\, dV \quad [33]$$

where the notation $\tilde{D} = (D^1 + 3h_0^2\, D^3)$ has been introduced. The expressions of K_T and K_ϕ are the same as in appendix I.2 excepted that D must be replaced by $\tilde{D}$ and $\tilde{B}_0$ by B_0 because of the new initial conditions.